Field-Controlled Photogeneration and Free-Carrier Transport in Amorphous Selenium Films

MARK D. TABAK AND PETER J. WARTER, JR.
Xerox Corporation, Rochester, New York
(Received 26 April 1968)

We have studied the photogeneration and transport of free carriers in amorphous selenium films under varying conditions of thickness, wavelength of the exciting radiation, and applied electric field. We have found that the efficiency of photogeneration is strongly field controlled, varying by two or more powers of 10 with the field changes reported. Using a technique based on time resolving the transport of free carriers across the film, we have measured deep-hole trapping times of 10–45 μsec and deep-electron trapping times of 40–50 μsec at room temperature. In addition, we have found hole-drift mobilities of 0.13–0.16 cm^2/V sec and electron-drift mobilities of 6.0–8.3×10^{-3} cm^2/V sec at room temperature, in good agreement with previous workers. These measurements allow an independent determination of the hole and electron range of $(1.3$–$6.3)\times10^{-6}$ cm^2/V and $(2.4$–$3.1)\times10^{-7}$ cm^2/V, respectively. The hole range measured in this new way is 20–100 times larger than previous determinations based on an inappropriate Hecht-type analysis, which is only a measure of the product of the generation and transport efficiency and not of the transport alone. The voltage dependence of the total transported charge cannot be described by a simple range limitation. The thickness scaling laws and the independent measurement of the range require that the photogeneration efficiency must depend on the applied electric field. It is suggested that the photogeneration step involves the field-aided thermal dissociation of a tightly bound hole-electron pair. This is indicated by the electric-field and wavelength dependence of the apparent quantum efficiency.

I. INTRODUCTION

THE study of the photogeneration and transport properties of amorphous selenium has been an area of active investigation, primarily because of the widespread use of this material in electrostatic imaging and also because of its interesting electrical and optical properties. In the xerographic form of imaging, a film of amorphous selenium is charged electrostatically and then exposed to light to form a latent image. The sensitivity of the discharge process that produces the latent image is directly related to the photogeneration and carrier-transport properties of the photoconductor material.

Previous measurements[1–3] of the voltage dependence of the rate of photodischarge of films of amorphous selenium have, for the most part, been interpreted in terms of bulk trapping of the mobile carrier, i.e., the photocurrent (or the rate of change of surface potential in a xerographic discharge) is limited by how *far* the free carriers move before they are trapped. The relevant parameter in such a model is the range, which is defined as the distance traveled per unit field and which in some cases can be conveniently thought of as the product of the drift mobility and the mean time to trapping ($\mu\tau$).

One of the objectives of this investigation has been to determine whether the observed voltage-dependent sensitivity can be ascribed to a range limitation. Such a description appears inconsistent with the ability to discharge fully a xerographic plate with very strongly absorbed radiation. If there were a bulk-transport limitation which significantly affected the photosensitivity, one would expect a large residual potential due to the trapped carriers, a property which has not been observed.

From the work being reported, we have found that the photocurrent-field characteristic cannot be described by a simple range limitation. *The observed scaling laws and an independent measurement of the range from transit-time data require that the photogeneration efficiency (i.e., the "quantum efficiency") must depend strongly on the electric field.*

The transient photocurrents produced by pulses of monochromatic light through evaporated films of amorphous selenium with blocking contacts can be used to measure the generation rate and the transport efficiency. When these measurements are performed as a function of applied field, wavelength, sample thickness, temperature, and light intensity, it is possible to evaluate the importance of various physical processes which might be responsible for controlling the photogeneration and transport properties. These results can be used to test the consistency of any proposed model and eliminate several alternatives.

A short description of the samples and the measurement technique is given in the next section on experimental details. The main results, divided into hole transport and photogeneration, electron transport and photogeneration, and quantum-efficiency measurements, are presented in the following three sections together with a critique of existing models in light of these results. In the final section a physical picture for the photogeneration process is discussed.

II. EXPERIMENTAL TECHNIQUE

The study of photoconductivity at high fields in insulating materials is often complicated by contact effects. Injection from the contacts can easily mask

[1] H. T. Li and P. J. Regensburger, J. Appl. Phys. 34, 1730 (1963).
[2] J. L. Hartke, Phys. Rev. 125, 1177 (1962).
[3] R. A. Fotland, J. Appl. Phys. 31, 1558 (1960).

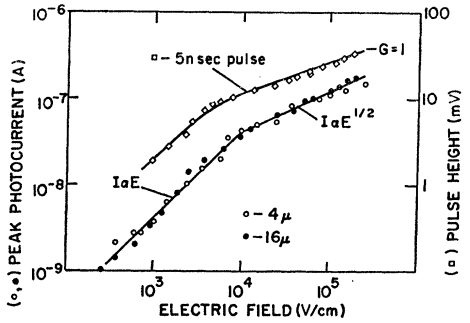

FIG. 1. The lower data show the hole-photocurrent–applied-field characteristic as a function of sample thickness for a 4300 Å msec light exposure. The upper curve gives the total voltage pulse height (integral of the current) as a function of the applied field for a 5 nsec exposure. The unity gain line shown corresponds to the photocurrent which would be obtained if each absorbed photon created a hole which went completely across the sample.

the fundamental photogeneration and transport processes being studied. It is possible to eliminate undesirable contact effects and maintain uniform high fields across the sample by using blocking electrodes and measuring the current-field curve with pulsed illumination. In using blocking contacts, however, care must be taken to avoid the effects of unneutralized space charge in altering the electric-field distribution. This technique has been described in detail in a previous publication.[4] A similar technique, but using pulsed electric fields, has been described by Many[5] in his study of high-field effects in cadmium sulfide.

If the duration of the light pulse is short compared to the time taken by the mobile carrier to drift across the sample, then, in addition to measuring the total charge transported, we can time resolve the drift of the mobile carriers across the sample. This technique, used by Hartke[2,6] and others for drift-mobility measurements, has been extended to include measurement of the bulk trapping times. Previous measurements by Blakney and Grunwald[7] have yielded information only on the electron-trapping parameters. By careful analysis of the pulse response we have been able to measure the hole-trapping parameters as well.

The transit-time signals are produced by using a 5-nsec light flash (generated by passing the output of a xenon flash lamp through a Kerr-cell shutter[6]) to inject a thin sheet of charge into a film of amorphous selenium with blocking contacts. By using a circuit time constant much larger than the transit time, we produced a voltage signal proportional to the time integral of the current and hence proportional to the charge induced on the electrodes.

The selenium films were prepared by evaporation of 99.99%-pure selenium, supplied by Canadian Copper Refiners, from an open boat at 250°C onto a KEL-F substrate held at 55°C at a pressure of about 5×10^{-5} Torr. The plastic KEL-F substrates were necessary to insure that the films adhere to the substrate at low temperature. The evaporated-gold electrodes used to apply the field were separated from the film by layers of an insulating plastic (Formvar) approximately 2000 Å thick. The thicknesses of the selenium films studied range from 2 to 108 μ.

III. HOLE PHOTOGENERATION AND TRANSPORT

The lower curve in Fig. 1 is a typical log-log plot of the hole photocurrent as a function of applied field at room temperature for two different sample thicknesses. These data were taken with millisecond light pulses, the peak photocurrent being recorded. The upper curve shows the voltage pulse height as a function of applied field, for hole transport, taken with a 5-nsec light flash and integrating the current. The voltage pulse height is directly proportional to the total transported charge and can also be shown to be directly proportional to the peak photocurrent. The advantage of using the short light pulse and measuring voltage change is that the transit time can be resolved. The applied field is calculated from the applied voltage and the geometry, and the illuminated surface is positively charged, so that the mobile carriers are holes. Care was taken to insure that the field was uniform across the sample by using depolarization techniques and resting the sample overnight between runs. Nonuniformities in the field could be detected by using the drift of the mobile carriers across the sample as a probe of the field distribution. The measurements reported

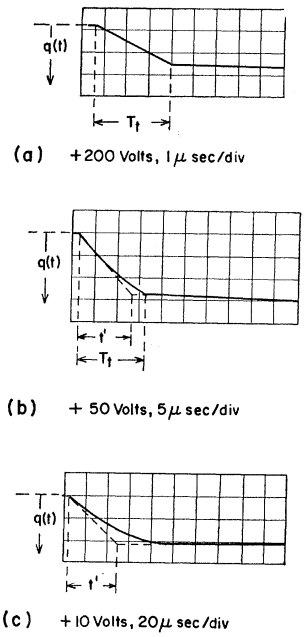

FIG. 2. Observed pulse shapes representing the charge displacement as the holes drift across the 108-μ sample. The applied voltage and time scale are shown below each trace: (a) high applied field, transit time $\approx\frac{1}{10}$ trapping lifetime, no trapping; (b) medium applied field, transit time $\approx\frac{1}{2}$ trapping time, some rounding due to trapping; (c) low-field case, no transit time observable, shape controlled by bulk trapping.

[4] M. D. Tabak, Trans. AIME **239**, 330 (1967).
[5] A. Many, J. Phys. Chem. Solids **26**, 575 (1965).
[6] J. L. Hartke and P. J. Regensburger, Phys. Rev. **139**, A970 (1965).
[7] R. M. Blakney and H. P. Grunwald, Phys. Rev. **159**, 664 (1967).

in this paper were made under conditions where there was no detectable evidence of initial trapped space charge. The photoexciting light was absorbed very near the illuminated contact, in all cases within a distance very small compared to the sample thickness. Therefore, if the illuminated surface is positively charged, the current will be determined by the photogeneration and transport of holes alone. One of the peculiarities of amorphous selenium is that it is not possible to create a detectable number of free carriers with weakly absorbed light, because of a large nonphotoconducting absorption in the visible range. A more detailed discussion of this nonphotoconducting absorption will be given in Sec. V.

The main features of both sets of data shown in Fig. 1 can be summarized as follows. At room temperature the current is a nearly linear function of applied field up to approximately 10^4 V/cm. Above 10^4 V/cm the rise in current with field is much less rapid, and in most samples the dependence of current on field is nearly a square-root dependence. In a few samples a less than square-root dependence was observed; slopes on a log-log plot of as low as 0.3 have been measured in the high-field region. The gain of one ($G=1$) line shown on Fig. 1 is the photocurrent which would be obtained if each incident photon (corrected for reflection losses) created one mobile hole which went completely across the sample.

Note that the current-field characteristic is independent of sample thickness for the same incident flux. These same features have also been observed in a xerographic-discharge experiment.[4] Although for clarity only two thicknesses are shown, the same curve fits data taken on a number of samples, ranging in thickness from 2 to 108 μ.

As mentioned in the Introduction, previous workers have usually interpreted the functional form of the above results in terms of a range limitation, which gives a relationship between current and voltage first developed by Gudden, Pohl, and Hecht[8] in the 1920's. The Hecht model simply states that the photocurrent is proportional to the average displacement of the free carriers divided by the sample thickness, when the average displacement is less than the sample thickness. The average distance traveled by a free carrier before trapping is called the schubweg and is given by $(\mu\tau)E$, where $(\mu\tau)$ is the range and E is the applied electric field. When the schubweg is equal to or greater than the sample thickness the photocurrent saturates, since the blocking electrodes do not allow secondary currents.

Previous measurements of the hole range have been made by fitting data of the type shown in Fig. 1 to a bulk-trapping model. We can check immediately whether a bulk-trapping model is appropriate by the thickness scaling laws of the current-field data. The lower curve in Fig. 1 shows that the current-field plot

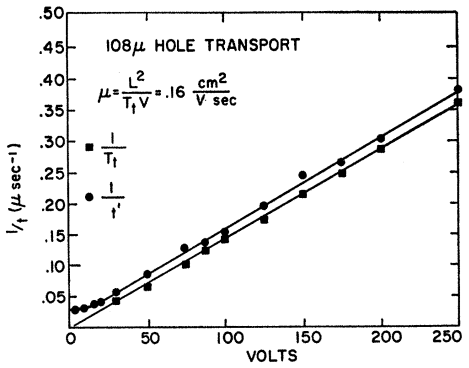

FIG. 3. Graphical technique for determining the value of the drift mobility from the slope of the $1/T_t$ line and for determining the bulk lifetime from the intercept of the $1/t'$ curve. The intercept of the $1/t'$ curve with the vertical axis gives a zero-field value of 34 μsec for t'.

is independent of sample thickness. If the range $\mu\tau$, which is a microscopic parameter, is to be independent of thickness, the scaling law appropriate to a bulk-transport-limited photocurrent is not satisfied, for in that case the current versus field/thickness should give a universal plot independent of sample thickness.

The range limitation becomes important when the schubweg $(\mu\tau)E$ is equal to or less than the sample thickness L. Since the transit time T_t of free carriers is given by $L/\mu E$, we should expect to see the effects of trapping when τ, the trapping time, is comparable to the transit time. Fitting a Hecht curve to the data in Fig. 1 produces a number for the hole range of approximately 5×10^{-8} cm^2/V. Dividing this by the value of the hole drift mobility[2] of 0.13 cm^2/V sec gives a number for the hole trapping lifetime of 0.4 μsec. However, as shown directly in Fig. 2, we can observe transit times for holes of the order of 10 μsec before any appreciable rounding of the transit-time pulse occurs due to trapping. *Clearly the decrease in photosensitivity with decreasing electric field is not due to a hole-trapping limitation at the fields shown in Fig. 1.*

It is possible to measure the true range, without reference to pulse height versus voltage data, by determining separately the drift mobility and the trapping time using a transit-time technique. Figure 2 shows the pulse shapes representing the integrated charge displacement as the holes drift across a 108-μ sample for three different values of applied field. The top picture shows the transit signal for 200 V applied, with a transit time of 3.5 μsec, without any rounding of the pulse. With 50 V applied, the transit time is 15 μsec and some slight rounding is evident. Finally, for 10 V applied, the signal is exponential with a time constant of 32 μsec, and a transit time cannot be defined.

The data are analyzed as follows: A transit time T_t is measured as shown in the upper and middle trace in Fig. 2. This fiduciary point, marked by an abrupt change in slope, can only be observed if a significant fraction of the carriers reach the opposite electrode at

[8] K. Hecht, Z. Physik **77**, 235 (1932).

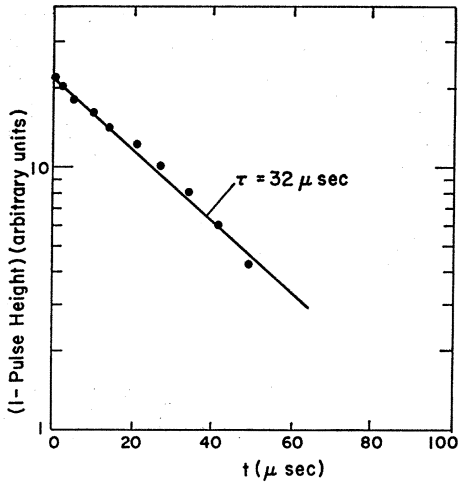

FIG. 4. Logarithm of the normalized value of the pulse response as a function of time showing the exponential nature of the low-field, lifetime-limited response.

one time. In addition, a time t' is also measured, defined by the intersection of the tangents to the pulse at $t=0$ and $t>T_t$, as shown in the middle and bottom traces.

Since the transit time is given by $L/\mu E$, a plot of $1/T_t$ versus the applied voltage should give a straight line with a slope of μ/L^2. Figure 3 shows the data for the 108-μ sample. The resulting straight line gives a value of 0.16 cm^2/V sec for the hole drift mobility. Also shown in Fig. 3 is $1/t'$ plotted as a function of the applied voltage. Notice that, at the lowest fields, t' saturates and becomes independent of voltage and intercepts the vertical axis at a value of 34 μsec. Figure 4 shows the time dependence of the signal [Fig. 2(c)] for 10 V applied plotted on a semilog scale. The functional form is exponential with a time constant of 32 μsec. The true hole lifetime is now unambiguously determined by both the intercept of the $1/t'$ plot and the time constant, as is shown by the analysis which follows.

The charge displacement for the trap-free case as a function of time is given by

$$q(t)=(\Delta Q\mu E/L)t, \quad t<T_t \tag{1}$$

and

$$q(t)=(\Delta Q\mu E/L)T_t, \quad t\geq T_t$$

where ΔQ denotes the total charge drawn out of the surface region. In the presence of a uniform volume distribution of deep-lying traps, the signal will become rounded as carriers are lost during the transit, the functional form being given by

$$q(t)=(\Delta Q\mu E\tau/L)(1-e^{-t/\tau}). \tag{2}$$

At $t=T_t$ the total charge displacement will be

$$q(T_t)=(\Delta Q\mu E\tau/L)(1-e^{-L/\mu E\tau}). \tag{3}$$

Following the procedure of Spear and Mort,[9] who used a similar method to determine the hole lifetime in CdS crystals, the intersection of the tangent to the curve at $t=0$ with the final value, which is experimentally defined by t', is given by

$$t'=\tau(1-e^{-T_t/\tau}). \tag{4}$$

When $T_t\gg\tau$, from Eq. (4), t' is equal to the lifetime. The time dependence of the charge displacement as given in Eq. (2) is exponential with a time constant also equal to the lifetime. The experimental results, shown in Figs. 3 and 4, verify these predictions. The time dependence is of exponential form with a time constant of 32 μsec, which is in excellent agreement with the value of 34 μsec determined from the intercept of the $1/t'$ plot in Fig. 3.

As an additional check, knowing the value of τ and using Eq. (4), we can calculate the value of T_t from the measured t'. Shown in Fig. 5 is a comparison of the calculated and measured value of $1/T_t$. The close agreement and the excellent linearity confirm the measurement of the hole lifetime and the validity of Eq. (4).

The true hole range can now be computed directly without reference to pulse-height data. The hole range is simply the product of the hole drift mobility and the lifetime and for this sample is equal to 5.1×10^{-6} cm^2/V.

Table I gives the results for four samples ranging from 16 to 108 μ in thickness. Samples M1 and M3 were prepared from the same batch of selenium shot, while S1 and A6 were made from different batches, all being supplied by Canadian Copper Refiners. The measured hole drift mobility ranges from 0.13 to 0.16 cm^2/V sec, in excellent agreement with Hartke[2] and Spear,[10] and the hole lifetimes vary from 10 to 45 μsec, giving a spread of $(1.3\text{–}6.3)\times10^{-6}$ cm^2/V in the calculated hole range. The hole-range values are 20–100

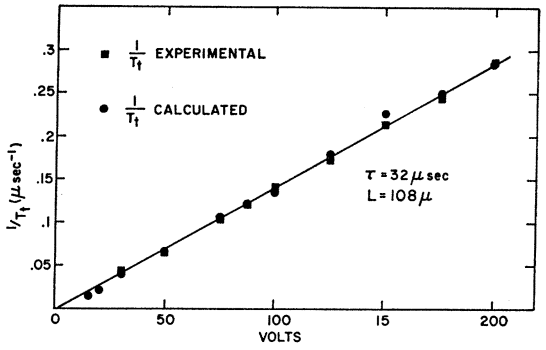

FIG. 5. Comparison between the experimentally determined values of the transit time and those calculated from the graphical intercept t' and the value of the bulk lifetime, using Eq. (4).

[9] W. E. Spear and J. Mort, Proc. Phys. Soc. (London) **81**, 130 (1963).

[10] W. E. Spear, Proc. Phys. Soc. (London) **B76**, 826 (1960); **B70**, 669 (1957).

TABLE I. Summary of room-temperature transport parameters for amorphous selenium films.

Sample	Thickness (μ)	Hole drift mobility (cm^2/V sec)	Hole lifetime (μsec)	Hole range (cm^2/V)	Electron drift mobility (cm^2/V sec)	Electron lifetime (μsec)	Electron range (cm^2/V)
S1	16	0.13	10	1.3×10^{-6}	6.3×10^{-3}	50	3.2×10^{-7}
M1	108	0.16	32	5.1×10^{-6}	...	...	...
M3	54	0.16	30	4.8×10^{-6}	8.3×10^{-3}	40	3.3×10^{-7}
A6	40	0.14	45	6.3×10^{-6}	6.0×10^{-3}	40	2.4×10^{-7}

times larger than those in the literature which were obtained by using the inappropriate Hecht-type analysis.

Since the decrease in photosensitivity with decreasing field is not due to trapping of holes during the transport, the number of carriers collected is being limited by processes operable in the region of carrier generation. Either the carrier generation rate depends on the electric field or the carriers are generated but then lost through a field-dependent recombination mechanism.

We have attempted to describe the field control of the net free-carrier generation by some recombination process. A very careful study of the many alternatives has convinced us that this is only possible if the recombination involves the hole and electron created by the absorption of a single photon. We choose to call this type of process *field-controlled photogeneration*, since true free carriers have never been created if separation has not occurred.

When considered together, the following collection of experimental facts rules out any explanation based on conventional recombination:

(1) The total charge transported depends only on the exposure (i.e., reciprocity applies) for changes in light intensity of six powers of ten and observations made on time scales from microseconds (where the transit times can be resolved) to many seconds (in a xerographic-discharge measurement). This linear behavior has also been reported by Blakney and Grunwald.[7]

(2) The structure of the photogeneration-field plot is not significantly affected by changes in the absorption constant, as shown in Fig. 6. This rules out any surface-recombination processes as discussed further below.

(3) Recombination centers in the absorption region would have to be very effective deep traps in the transport region (i.e., the bulk). These are not observed. Note that there could not be a fortuitous concentration of recombination centers in the absorption region consistent with the changes in absorption depth indicated in Fig. 6, for what is the absorption region at long wavelengths is a transport region at shorter wavelengths.

A number of measurements have been made to define the role of the surface in determining the form of the photogeneration-field characteristic. At the higher fields, the potential difference between the points where the photons are absorbed and the surface is many times (kT/e). Thus, for the high fields, the diffusion to the surface of a charged carrier of the same sign as the surface charge is extremely unlikely. At fields below 10^4 V/cm, and for strongly absorbed light, diffusion of a charged carrier to the surface would be probable. If this were relevant to the change in slope of the photogeneration-field plot at approximately 10^4 V/cm, then the critical field should shift with changes in the absorption constant. As indicated in Fig. 6, this is not observed.

A number of chemical surface treatments which are known to increase or decrease the xerographic-charge acceptance have been tried, and samples have been subjected to varying degrees of mechanical abrasion. *None of the surface modification tried, short of mechanical damage to a depth greater than the absorption depth, has any effect on the photogeneration-field characteristic.* We feel that this argues against the possibility of surface decay or dissociation of *uncharged* photoexcited pairs which have diffused to the surface.

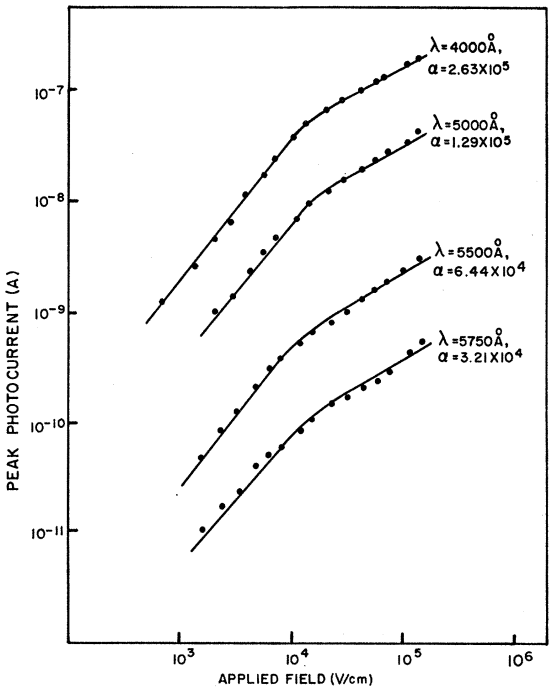

FIG. 6. Hole photocurrent versus applied field for different values of the wavelength of the exciting radiation.

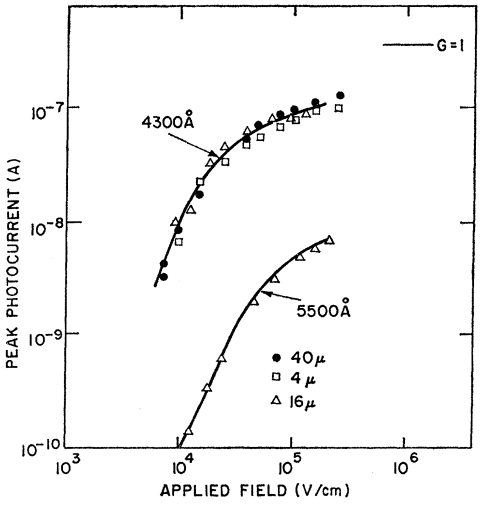

FIG. 7. Electron photocurrent versus applied field showing the thickness scaling laws and the long- and short-wavelength response.

IV. ELECTRON PHOTOGENERATION AND TRANSPORT

The electron photocurrent was measured in the same way by simply making the illuminated surface negative. It was again observed that the variation in sensitivity with voltage was not bulk-transport (range) controlled. The same scaling laws hold as for the hole case as indicated in Fig. 7. *Again the photogeneration of electrons is field-controlled.*

The interpretation of the electron photogeneration curves is complicated by the comparatively small electron range as discussed below. Because of this, the electron situation is not nearly as clearly defined.

As shown in Fig. 7, the electron photogeneration curve is much steeper than the hole photogeneration curve at low fields, and the fall off begins at higher fields for the electron case. Also shown in Fig. 7 is a typical long-wavelength (5500 Å) response which has generally the same shape as the 4300 Å response. Following the reasoning presented above, these data would seem to rule out surface effects as the source for the low-voltage electron-hole asymmetry. It should also be noted that a small (20% maximum) electron-hole asymmetry in quantum efficiency is often observed at the higher fields which remains an anomaly in the data in spite of very careful efforts to remove any experimental uncertainty.

Following the procedures discussed for holes, the electron-transport properties were measured. The only change necessary was to make the illuminated surface negative, so that electrons are drifted across the sample. The results of this experiment are shown in the second half of Table I.

The electron drift mobilities range from 6.0 to 8.3 $\times 10^{-3}$ cm^2/V sec, again in excellent agreement with Hartke[2] and Spear.[10] The drift mobility for sample M1 could not be measured reliably, since it was too thick to observe well-defined transit times. The electron lifetimes varied between 40 and 50 μsec. These numbers can be compared to the recent results of Blakney and Grunwald,[7] who found two separate time constants, one in the neighborhood of 5 μsec and another at about 20–30 μsec. We have not observed the fast component in well-rested samples (shorted in dark for 12 h). Samples which were not rested showed such an apparent fast component, which we were able to relate to the presence of trapped holes, which will give rise to an increase in the field near the illuminated surface. Under these nonuniform field conditions the plot of inverse transit time versus applied voltage should not go through the origin. We have observed this behavior in the non-well-rested samples which showed the fast component, and Grunwald[11] also observed this effect in his samples.

The calculated electron range varied between 2.4 and 3.3×10^{-7} cm^2/V. These numbers may be compared to those found from pulse-height analysis by Regensburger[12] [$(5.0\text{–}8.3)\times10^{-8}$ cm^2/V] and Hartke[2] [$(1\text{–}2)\times10^{-7}$ cm^2/V]. The agreement between the electron range as derived from pulse-height analysis and from transit-time analysis is much closer for the electrons than for holes, which simply indicates that electron trapping is more effective than hole trapping in limiting the photosensitivity. For example, a 50-μ sample would show evidence of electron trapping at a field of 2.5×10^4 V/cm, while the hole transport should be trap-free down to fields of 1×10^3 V/cm.

V. QUANTUM-EFFICIENCY MEASUREMENTS

In amorphous selenium a gap exists between the optical-absorption edge and the photoconductive edge. Hartke and Regensburger[6] have shown that the absorption coefficient falls off exponentially for wavelengths greater than 5600 Å, while the relative photoresponse starts to fall off at 4500 Å. If the optical absorption corresponds to band-to-band transitions, one would expect the absorption and photoresponse edges to coincide. In fact, the photoresponse starts to fall off about 0.6 eV higher than the optical absorption. Several models for this effect have been proposed. Lanyon[13] has postulated that this behavior is due to transitions from filled states lying below the Fermi level to the conduction band. These transitions would produce optical absorption and electron photoconductivity but no hole photoconductivity, since the hole would be trapped in a bound state. Accordingly, as pointed out by Hartke and Regensburger, the quantum efficiencies for holes would be much lower than that for electrons in the spectral region between the absorption edge and the photoconductive edge. Hartke and

[11] H. P. Grunwald, Ph.D. thesis, University of Rochester, Rochester, N. Y., 1966 (unpublished).
[12] P. J. Regensburger, J. Appl. Phys. **35**, 1863 (1964).
[13] H. P. D. Lanyon, Phys. Rev. **130**, 134 (1963).

Regensburger experimentally found nearly equal quantum efficiencies for the holes and electrons and formulated their explanation in terms of intrinsic exciton absorption. Recently, Siemsen and Fenton[14] have presented optical data that support the postulate of Hartke and Regensburger. However, low-temperature measurements by Tutihasi[15] have not revealed the existence of structure in the optical absorption that would be expected from an exciton absorption. We have found that the "photoconductive edge" shifts toward longer wavelengths with increases in the applied field. The quantum efficiency increases quite rapidly with increasing applied field (above 10^5 V/cm) for wavelengths longer than 4500 Å. We can illustrate this effect by reference to previous measurements and our results presented later.

Figure 8 shows a summary of previous work on the quantum efficiency[3,16–19] as a function of wavelength, taken from the paper of Hartke and Regensburger. The agreement between different workers is not particularly good. One reason for the poor agreement is that, in order to measure a true quantum efficiency, it is imperative that the photoresponse-applied field curve be saturated; otherwise a change in the field produces a change in the measured quantum efficiency. Since saturation is never observed, one must extrapolate the data, using an assumed model such as a range limitation, to arrive at the true quantum efficiency. Most of the data shown in Fig. 8 were taken at some arbitrary field with no correction made for the fact that photoresponse-field curve was not saturated.

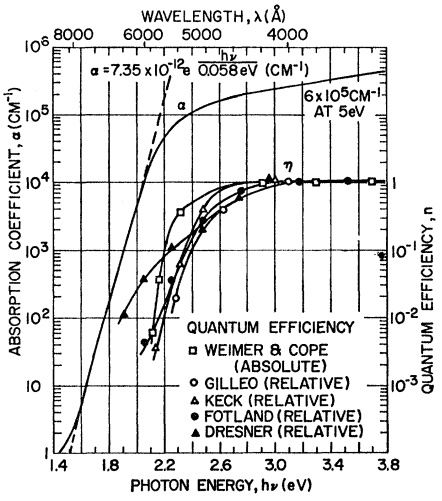

FIG. 8. Quantum efficiency and optical absorption measurements for amorphous selenium at room temperature (after Hartke and Regensburger, Ref. 6).

[14] K. J. Siemsen and E. W. Fenton, Phys. Rev. **161**, 632 (1967).
[15] S. Tutihasi (private communication).
[16] P. K. Weimer and A. D. Cope, RCA Rev. **12**, 314 (1951).
[17] M. A. Gilleo, J. Chem. Phys. **19**, 1291 (1951).
[18] P. H. Keck, J. Opt. Soc. Am. **42**, 221 (1952).
[19] J. Dresner, J. Chem. Phys. **35**, 1628 (1961).

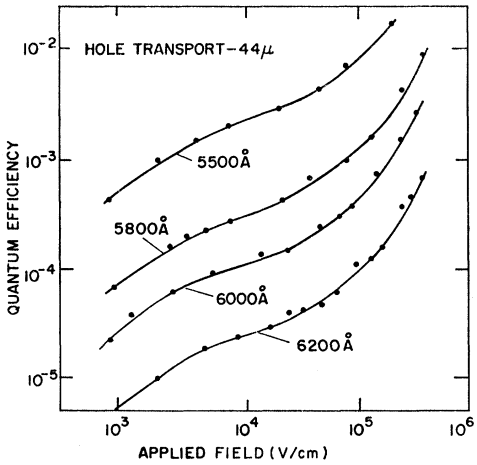

FIG. 9. Hole quantum efficiency versus electric field for long-wavelength excitation using a xerographic-discharge technique. The rapid turnup for fields greater than 10^5 V/cm corresponds to a shift of the "photoresponse edge" toward lower photon energies.

Weimer and Cope[16] used a vidicon scanning technique, with an applied field of $\sim 10^5$ V/cm, while the other data were taken at much lower fields, using sandwich-cell geometry. Weimer and Cope's data show a much higher quantum efficiency for the long wavelengths.

Our results, presented in Fig. 9, illustrate this rapid increase of the hole quantum efficiency with applied field for the long-wavelength irradiation. These measurements were made xerographically, so that fields up to 4×10^5 V/cm could be applied; conventional electroded sandwich structures fail at fields above 1.5×10^5 V/cm. In a xerographic-discharge experiment one measures the rate of change of surface potential at $t=0$, which is directly proportional to the photocurrent in a constant-voltage experiment.[4] This rapid change in apparent quantum efficiency with increasing applied field is only observed for wavelengths longer than 4500 Å and has the effect of shifting the photoresponse edge toward the lower energies. In the next section we will show that this behavior is consistent with current thinking on a field-controlled photogeneration mechanism, where an increase in the field can lead to an exponential increase in the number of carriers generated.

Temperature Dependence

The temperature dependence of the hole photocurrent as a function of applied field, as shown in Fig. 10, illustrates some interesting features. One finds that the photocurrent is quite sensitive to temperature in the low-field region, decreasing exponentially with decreasing temperature, and that the dependence on temperature decreases as the applied field is raised. The activation energy decreases from approximately 0.12 eV at 2.0×10^3 V/cm to 0.034 eV at 2.5×10^4 V/cm.

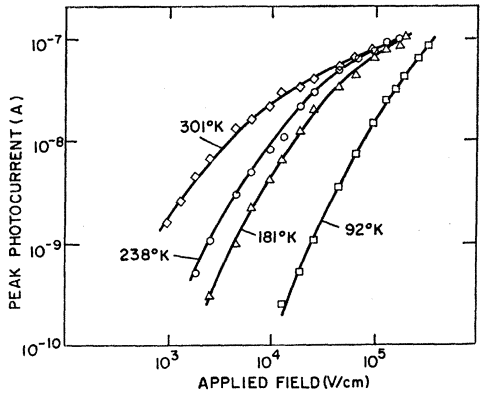

FIG. 10. Temperature dependence of the hole-photocurrent–applied-field characteristic for 4300 Å exciting radiation.

It is clear that this type of behavior is also not characteristic of a bulk-transport limitation.

In Sec. VI we will show that this behavior may be described in terms of the temperature dependence of the photogeneration mechanism, where the rate of generation is thermally activated and aided by the electric field.

VI. DISCUSSION

The previous results have demonstrated that a conventional range-limited model cannot explain the photoconductive response of amorphous selenium. The available evidence suggests that the most consistent explanation for the photodischarge properties can be found in a model that postulates that the *supply* of carriers available for transport is a function of the applied field.

In the following paragraphs we would like to suggest a physical picture for the photogeneration process and show how it is related to the processes in molecular solids. *While the following discussion is not rigorous or complete*, it is presented in the hope of shedding more light and generating more insight into the photogeneration process.

We feel that the photoelectronic properties of amorphous selenium are those of a molecular solid where the excitation occurs within a molecule and the transport between molecules is governed by the comparatively weak overlap between molecular wave functions. For example, in anthracene, a typical molecular crystal, it has long been recognized that a localized excited state is the intermediate step between the absorption of a photon and the production of a free carrier pair.

In order to account for the experimental results, one can consider that the photon produces a localized excitation that can be generally described in terms of a tightly bound hole-electron pair. It is convenient to lump all the processes for decay of the excitation into two fundamental channels, one channel giving free carriers and the other encompassing all the nonphotoconductive decay processes. In this latter channel, the excitation may decay by interaction with phonons, dislocations, or defects, giving up its energy of formation in vibrational energy or, in some cases, radiation. Competing with this decay process is the dissociation of the excitation into a free hole-electron pair by action of an applied field, phonons, collisions, or a combination of these effects. The decay of the excitation into vibrational energy might possibly account for the nonphotoconducting absorption in the spectrum of amorphous selenium.

Direct electric-field ionization will only occur when the potential-energy difference across the diameter of the orbit is of the order of magnitude of the binding energy of a particle in the orbit. One finds that, for a tightly bound hole-electron pair (e.g., a Frenkel exciton), the field necessary for direct ionization is much too high to explain our results. It is also possible to ionize the excitation by a field-aided thermal process, where the energy for ionization is supplied by the phonons but the barrier is lowered by the applied field. The formalism is essentially that of the Poole-Frenkel[20] effect, i.e., the lowering of a Coulombic barrier by the action of an applied field. The following simple calculation shows how this effect might be applied to our experiment.

Two additions to the simple Poole-Frenkel effect are necessary to apply it to this case. First, the maximum rate at which free carriers are formed must be limited by the incident photon flux, since the quantum efficiency cannot exceed unity. Secondly, a nonphotoconductive transition for the decay of the excitation must be provided which competes with the decay of the excitation into a free hole-electron pair. The steady-state rate equation for this model is

$$dN/dt = g_p - N/\tau_r - N/\tau_i = 0, \tag{5}$$

where N is the excitation density, g_p is the excitation generation rate, which is directly proportional to the incident photon flux, $1/\tau_r$ is the rate of nonphotoconductive decay of an excitation, and $1/\tau_i$ is the rate that the excitation will dissociate into a free hole-electron pair. Since the generation rate of free hole-electron pairs is N/τ_i, the quantum efficiency is given by

$$\eta = \frac{N/\tau_i}{g_p} = \frac{1}{1+\tau_i/\tau_r}. \tag{6}$$

The probability for ionization of the excitation can be described by a thermally activated process, with an activation energy which can be reduced by an increase in the applied electric field. If it is a Coulombic barrier which is lowered by the field, then

$$1/\tau_i = \nu e^{-\xi_i/kT} e^{+e\Delta V/kT}, \tag{7}$$

where $\Delta V = (eE_0/\pi\epsilon)^{1/2} = \beta E_0^{1/2}$, ν is the attempt-to-

[20] J. Frenkel, Tech. Phys. USSR 5, 685 (1938); Phys. Rev. 54, 647 (1938).

escape frequency, ξ_t is the binding energy of the excitation, ϵ is the dielectric constant, and E_0 is the applied field.

The quantum efficiency for this model can now be written as

$$\eta=\left[1+\frac{1}{\tau_r\nu}\exp\left(\frac{\xi_t-e\beta E_0^{1/2}}{kT}\right)\right]^{-1}. \quad (8)$$

Figure 11 shows the form this expression takes for several temperatures. The binding energy ξ_t in this example is taken to be 0.1 eV and $(1/\tau_r\nu)\exp(\xi_t/kT)$ is set equal to 10 at 300°K to give correspondence with the experimental results of Fig. 10. Except for the region below 10^4 V/cm, which we will discuss later, there is a reasonable qualitative agreement between Eq. (8) and the experimental results. The slope of the curve increases with decreasing temperature and the activation energy depends on the square root of the applied field for values of field greater than 10^4 V/cm. Below 10^4 V/cm, Eq. (8) predicts that the quantum efficiency will approach a nonzero value as the field goes to zero, while experimentally we observe the quantum efficiency dropping quite rapidly with decreasing field. It is thus clear that the modified Poole-Frenkel model cannot describe the low-field behavior. The field for which the modified Poole-Frenkel saturates at the low-field end is that for which the barrier lowering is of the order of (kT/e). It is at this point that other thermally driven processes may be expected to dominate.

In this calculation we have only tried to show that a simple model of field-aided thermal dissociation to produce free carriers can qualitatively explain several features of the photogeneration characteristics. Another discussion of this model relative to amorphous selenium has been given recently by Pai and Ing.[21] Their results show that the functional form of the pulse height versus voltage data and the activation energies derived from the analysis fit reasonably well to the simple unmodified Poole-Frenkel expression $[i\sim\exp(e\beta E_0^{1/2}/kT)]$ for the longest wavelengths, although there is no agreement at shorter wavelengths. This same expression also fits the high-field part of our data shown in Fig. 9.

We consider that this long-wavelength correlation supports the position that the field-dependent photogeneration mechanism involves a field-aided thermal dissociation step. In order to fit the long-wavelength data with an $\exp(\beta E_0^{1/2})$ curve, Pai and Ing had to assume a value of β one-half of that which one would expect for the simple Poole-Frenkel model. The use of such a modified β would give better high-field agreement between our model and the short-wavelength

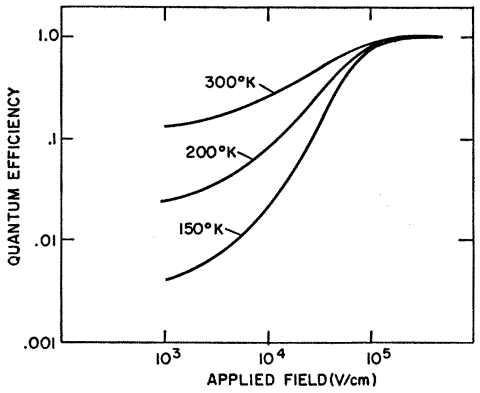

FIG. 11. Plot of Eq. (8) showing the field dependence of the quantum efficiency for three different temperatures.

data than that indicated in Fig. 11, where we have simply used the dc dielectric constant in computing β. It has been suggested by Hartke[22] that the β appropriate to a three-dimensional Poole-Frenkel model may be reduced by as much as a factor of 2 from the standard (one-dimensional) expression. A factor of 2 change in β would shift the curves of Fig. 11 to fields four times higher. It should also be noted that values of β a factor of 2 lower than predicted are very often observed[23] in insulators showing a transport limitation varying as $\exp(\beta E_0^{1/2})$. This anomaly has not been resolved even though it has been the subject of much discussion.

Pai and Ing have shown that the hole photogeneration, at room temperature and at wavelengths longer than 5600 Å, is directly proportional to $\exp(\beta E_0^{1/2})$ for fields above 10^4 V/cm. This means that the field-thermal excitation for these longer wavelengths must be from a somewhat deeper level than the excitation for the shorter wavelengths discussed above. This is necessary to allow for the relatively rapid increase in photogeneration efficiency with field at the highest fields and longest wavelengths. This is supported by the thermal-activation measurements of Pai and Ing, who found the activation energy increasing with increasing wavelength.

ACKNOWLEDGMENTS

The authors are particularly grateful to Dr. Fred Schmidlin for suggesting the calculation of quantum efficiency using a competing-lifetime approach. We are also grateful to J. Neyhart for allowing us to use some of his xerographic-discharge measurements. It is a pleasure to acknowledge the many helpful discussions with Dr. J. Mort and Dr. E. A. Davis. The assistance of M. Scharfe and D. Georgenson in performing many of the measurements is appreciated.

[21] D. Pai and S. W. Ing, Phys. Rev. 173, 729 (1968).

[22] J. L. Hartke (to be published).

[23] A. K. Jonscher, Thin Solid Films 1, 213 (1967).